Compaction of a Bed of Fragmentable UO_2 Particles and Associated Acoustic Emission

L. Hégron, P. Sornay, and N. Favretto-Cristini

***Abstract*—The nuclear fuel of light water power reactors is manufactured by powder metallurgy. This method is also used for the production of fuels containing minor actinides which have high activity and long life. Given their radiotoxicity, maximum simplification in the manufacturing process is necessary in order to limit dissemination and retention of matter. In addition to this, the fuel must have a mostly open porosity. Implementation of particles of a few hundred micrometers and controlled cohesion could achieve this dual objective. However, the mechanical strength of compacts before sintering must be sufficient without adding binder. The phenomena which occur during the manufacturing of compacts are thus analyzed and quantified. We show that only a part of the particles breaks upon application of a stress of up to 600 MPa and it is possible to detect this fragmentation by acoustic emission (AE).**

***Index Terms*—Acoustic emission, compaction, granular material, porosity, UO_2 .**

I. Introduction

CURRENT nuclear fuel manufacturing implements a powder metallurgy process which consists of three main steps: preparation of the powders, their compaction, and sintering of the compact. It is also the reference process for the production of fuels containing minor actinides with high activity and long life which are intended to be used in the fourth generation reactors. However, given the radiotoxicity of these fuels, they can be manufactured only in shielded cells. It is therefore necessary to simplify the manufacturing process as much as possible thereby limiting dissemination and retention of nuclear matter. The technique which controls the process should be easy to implement and robust in a hostile and hardly reachable environment. In addition, in order to facilitate the release of helium during irradiation, one solution is to create a fuel with a porosity essentially open after sintering. That means that a majority of the pores are connected to the outside of the pellet.

Instead of the micronic powders currently used for the production of fuels, the use of particles of a few hundred micrometers, graded in size, shape and cohesion, should thus help to limit the dissemination and retention of the nuclear matter. Such particles also facilitate the filling of the press die. Nevertheless, the implementation of large particles without addition of an organic binder can lead to a compact which does not permit mechanical handling in the industrial manufacturing process. An optimum between size, shape and cohesion of the particles must be sought to obtain a compact with sufficient mechanical strength, while respecting the specifications of the sintered product. It is therefore appropriate to identify and quantify the mechanisms which occur during compaction according to the characteristics of compacted particles. We are interested in highlighting more specifically the mechanism of particle fragmentation. We present the evolution of the compactness of a particle bed, depending on the applied stress. We then observe the microstructure of compacts with different compactness values. Finally, we analyze the acoustic emission (AE) generated by the fragmentation of a single particle and that generated by a particle bed during compaction. This technique, already used to monitor the compaction of pharmaceutical powders [1]–[3] has the advantage of being simple to adapt to nuclear-oriented purposes.

Manuscript received August 05, 2013; revised November 25, 2013; accepted January 09, 2014. Date of publication March 07, 2014; date of current version August 14, 2014.

L. Hégron and P. Sornay are with CEA, DEN, DEC, SPUA, LCU, F-13108 Saint Paul Lez Durance, France (e-mail: l.hegron@gmail.fr; philippe.sornay@cea.fr).

N. Favretto-Cristini is with LMA, CNRS UPR7051, Aix-Marseille Université, Centrale Marseille, 13402 Marseille Cedex 20, France (e-mail: favretto@lma.cnrs-mrs.fr).

Color versions of one or more of the figures in this paper are available online at http://ieeexplore.ieee.org.

Digital Object Identifier 10.1109/TNS.2014.2300702

II. Material and Experimental Setup

A. Uranium Dioxide (UO_2) Granules

Studies [4] to obtain calibrated particles directly during the manufacturing of actinide oxides are now in progress. Nevertheless, the particles which are implemented in our study are obtained by mechanical granulation of UO_2 powder. They are obtained by compaction of a powder at the pressure 600 MPa; the elementary particles are submicron. The compacts are then crushed and size sorting is performed to keep only particles ranging between 160 and 500 micrometers. These particles are called granules. The density of the compact, determined by weighing and measurement, is $6.45\ g/cm^3$, which corresponds to a compactness of 59%. The granules also have this density. They have a polyhedral shape, as shown in Fig. 1(a). Given the method for obtaining granules, some of them may have dimensions greater than 500 micrometers. Their observation at higher magnification allows visualization of the powder particles constituting the granules [Fig. 1(b) and Fig. 1(c)]. Links which bind these particles are Van der Waals attractions, electrostatic forces and capillary forces [5]. The dendritic shape of the powder particles also contributes to the cohesion of the granules [6].

B. Compression System and Acoustic Emission Line

The granules are poured into the press die and are compacted between two punches with a diameter of 10 mm (Fig. 2). The upper punch can move and the lower punch is fixed. The die

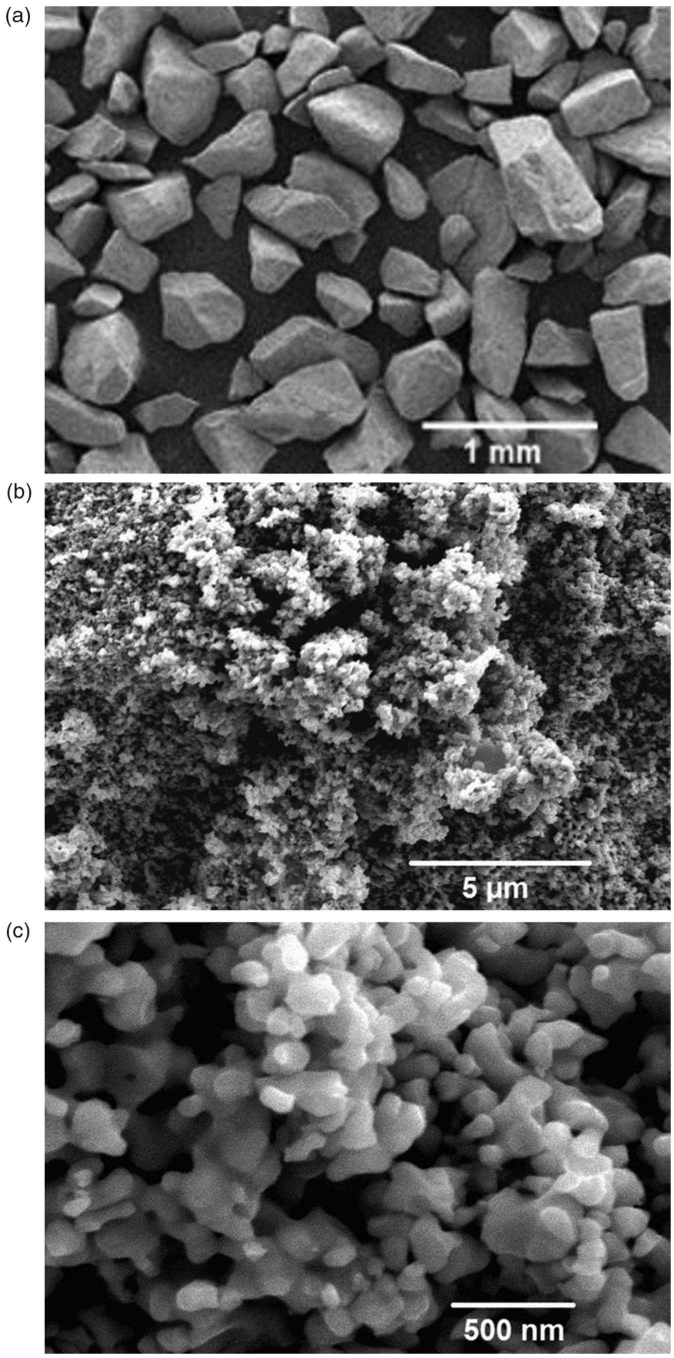

Fig. 1. SEM observations of UO_2 granules (600 MPa, 160-500 μm) at various magnifications.

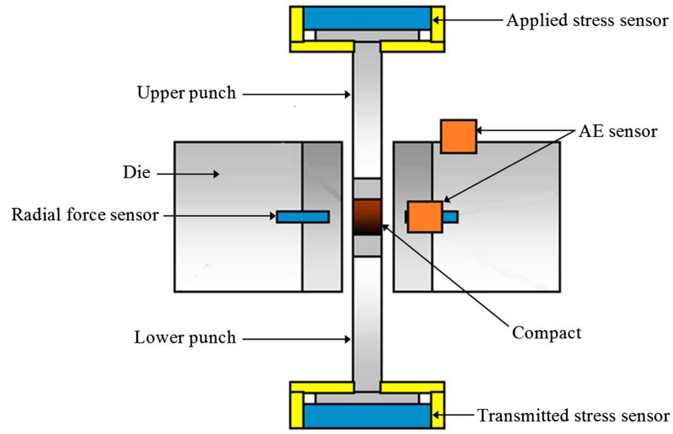

Fig. 2. Diagram of the compression system with force sensors and acoustic emission sensors.

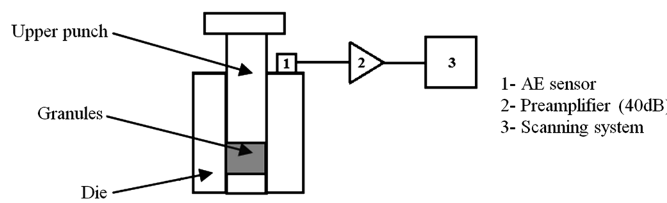

Fig. 3. Diagram of the acoustic emission record system.

is mobile, which allows ejection of the compact. Compaction is carried out at a speed of 0.1 mm/s for the movement of the upper punch until reaching the desired applied stress. This pressure is then maintained for 15 seconds before being reduced. During the ejection, a pressure approximately ten times lower than the maximum applied stress is maintained on the compact. That controls the release of stored elastic energy during compaction, which avoids cracking or delamination of the compact [7], [8]. Force sensors (in blue in Fig. 2) are arranged directly on the punches and in the die. They record the force applied on the upper punch, the force transmitted to the lower punch and the radial force applied by the powder on the die. These three forces are used to calculate the friction coefficient between the granules and the die and the ability of the granules to convert an axial force into a radial force. The average stress viewed by the compact is equal to the geometric mean of the applied stress and the transmitted stress [9]. Knowing the strengths, the position of the upper punch at any time and the compliance of the press, we can calculate the variation in height of the compact as a function of stress.

Furthermore, the die is equipped with two piezoelectric sensors (in red in Fig. 2). They record the acoustic emission (AE) during compaction using a device developed by the Mistras Company (Fig. 3). AE sensors have a frequency bandwidth between 100 kHz and 1 MHz. To enhance the signal transmission between the die and the sensor, they are fixed to the die by means of a spring which ensures a constant holding force. Silicon grease is used as a couplant. Before each test series, we test the quality of the sensor mounting by recording the acoustic emission produced by a pencil lead break as described in the norm “NF EN 1330-9”.

Fig. 4 shows a typical burst signal of acoustic emission and some associated parameters. The straight forward parameter is the number of hits, i.e. the number of pulses which exceed the detection threshold. It is not possible to associate the number of hits to a particular phenomenon because of the diversity of emission origins in the compact (friction, fragmentation), and possible spurious noise (background noise, electromagnetic radiation, mechanical vibrations related to the machine). An acoustic emission caused by a given mechanism will however lead to a typical burst signal shape.

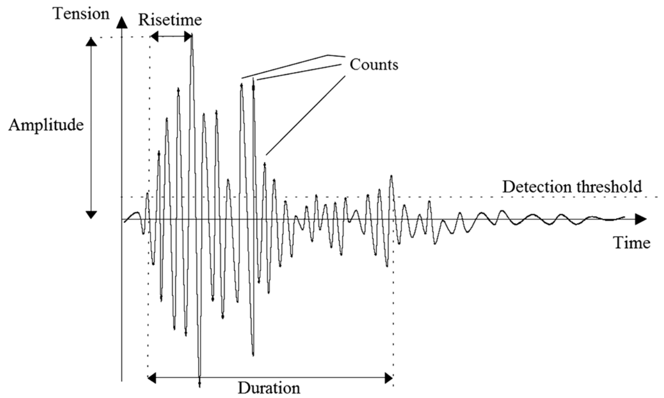

Fig. 4. Burst signal parameters.

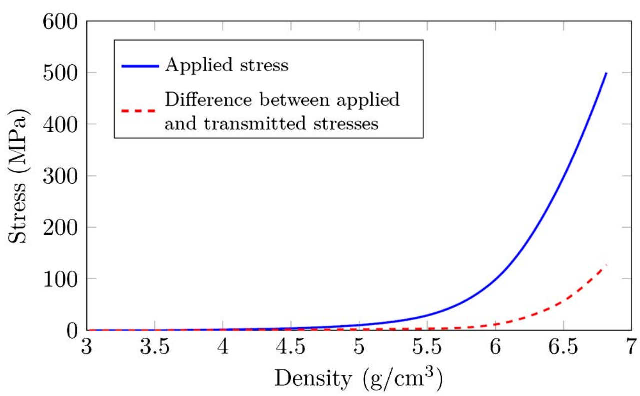

Fig. 5. Evolution of the applied stress and the difference between the applied stress and the transmitted stress as a function of the density.

III. Results

A. Evolution of Porosity During Compaction

Knowing the mass of granules introduced into the die, it is possible to monitor continuously the density of the compact of UO_2 granules as a function of applied stress. The density after filling the die is 3.0 g/cm^3, which corresponds to a compactness of 47% of the stack of granules. The applied stress (Fig. 5) varies between 0 and 1 MPa (the interval corresponding to the measuring accuracy of force) as the density is less than 3.9 g/cm^3 (compactness of 60%).

We can note that the stress rapidly increases beyond about 40 MPa which corresponds to a density in the die of 5.7 g/cm^3. Beyond 40 MPa, the difference between the applied and transmitted stresses also becomes significant. The density monotonically increases with stress. It is not possible to discern from this curve change in the compaction mechanism. After ejection, the density of the compact compressed at 600 MPa is 6.80 g/cm^3; the rebound occurring during ejection is of the order of 8%. Moreover, we find that this density is greater than the measured density for the powder compacted at the same stress (6.45 g/cm^3).

Observation of a ceramographic section of compacts performed at different applied stresses allows us to visualize the evolution of the microstructure (Fig. 6). After the application of a stress of 5 MPa, there are cracked granules and large porosity between the granules. Fragments of cracked granules will facilitate the rearrangement of granules. It seems that some granules are very fragmented while others are almost unfragmented.

When the stress increases from 5 MPa to a value between 100 and 300 MPa, fragmentation increases. Between 300 and 600 MPa, the size of the granules does not however vary greatly. The difference in granular appearance on the picture of compacts formed at 5, 20 and 60 MPa and those formed at 100, 300 and 600 MPa is due to sample preparation. The former compacts are embedded in resin under vacuum and then polished, while the latter are thermally consolidated before being polished.

Even after an applied stress of 600 MPa, there are still some spaces between the granules which are not filled. These spaces are not due to granule wrenching during preparation of the sample, but to pores existing in the compact. It can be concluded that some granules may be subjected to high isostatic loads and low shear stress. They do not fragment and as a result, the porosity between the granules is not completely reduced.

Quantification of granule size by image analysis is undergoing. A first data analysis enabled us to calculate the porosity between the granules. For low applied stresses, it can be assumed that the granules themselves do not densify. We can then evaluate the porosity between the granules by calculating the density of the compact and the density of the granules (6.45 g/cm^3).

As expected, porosity decreases as the stress increases (Fig. 7). The error bars are related to the uncertainty in the measurement technique. For a stress of 400 MPa, the density of the compact is equal to that of the granules. The granules significantly densify on themselves at a stress of 400 MPa. Therefore, the assumption made to calculate the porosity between the granules is no longer valid. It is the reason why the calculated porosity between the granules of compacts at 600 MPa is negative. It remains true that the porosity rate thus calculated is comparable to that determined from the image analysis. For stresses below a hundred MPa, which should not lead to a significant densification of the granules on themselves, the observed differences may come from a too low sampling measurement by image analysis.

Analysis by mercury intrusion porosimetry [10] of compacts would reveal the size of the pores. However, if this method is used to identify the stress from which the volume of pores between the granules becomes negligible, it cannot monitor/detect granule fragmentation. Only observations of the microstructure of compacts show that granule fragmentation occurs for stresses below 300 MPa.

B. Acoustic Emission During Granule Compaction

Acoustic emission is used in many processes as a passive technique to monitor real-time processes which emit acoustic waves. This technique is particularly used to detect and/or monitor cracks in materials. For example, Kerboul [11] followed the formation of cracks which sometimes occurs during the ejection of actinide powder compacts. In our case, the objective is to detect in situ fragmentation of granules to infer the evolution of the microstructure. Before studying the acoustic emission during compaction of a bed of granules, we crushed a single granule.

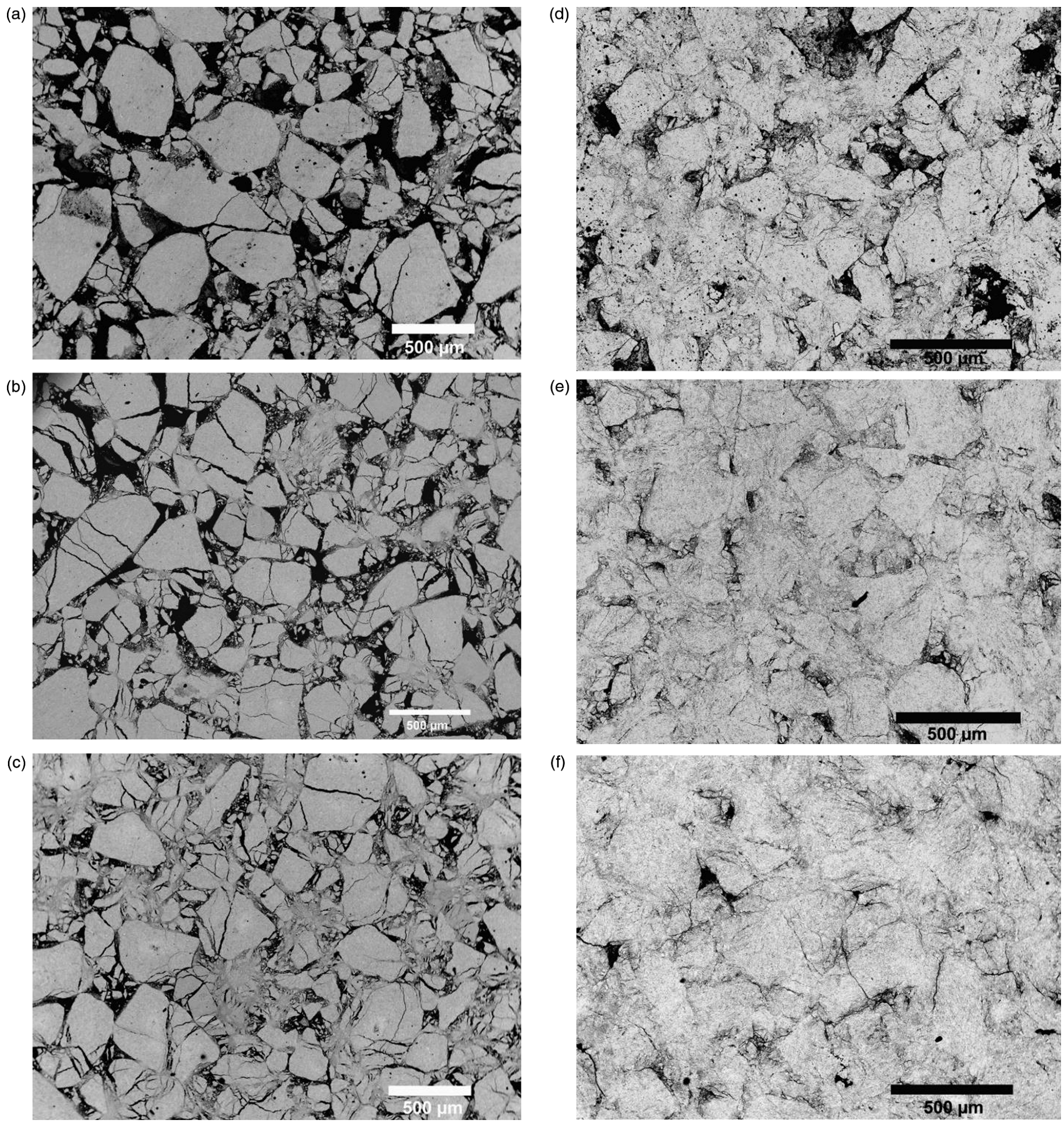

Fig. 6. Ceramographic sections of compacts of granules performed at: (a) 5 MPa, (b) 20 MPa, (c) 60 MPa, (d) 100 MPa, (e) 300 MPa, (f) 600 MPa.

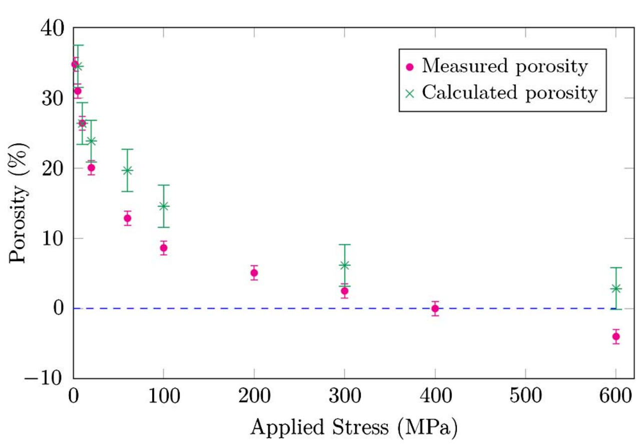

Fig. 7. Evolution of the porosity calculated by weighing and geometric measurements and the porosity measured by image analysis, as a function of the applied stress.

1) Crushing of a Single Granule: One granule is crushed between two punches with a diameter of 3 mm (Fig. 8). The speed of the upper punch is 500 μm/min and the lower punch is fixed. The load curve is represented in Fig. 8. The force first gradually increases and then abruptly decreases. The granule then has a crack. The maximum force which is the breaking strength is $1.5\ \mathrm{N} \pm 0.7\ \mathrm{N}$ (dispersion obtained for a 15 granule batch). The displacement to achieve the breaking strength is approximately 80 micrometers. It corresponds to the formation of flat surfaces on the granule in contact with the punches and deformation of the granule.

We simultaneously record acoustic emission with an AE sensor fixed near the lower punch. During the increase in stress, no acoustic emission exceeds the threshold which was fixed at 25 dB. Upon breakage, a single event characterized by the acoustic burst signal shown in Fig. 9(a) is detected. This waveform is the typical signal of the fracture, regardless of the surface on which the punch is touching. It has a shape similar to a graphite pencil lead break [Fig. 9(b)]: a fast rise time followed by an exponential decay. Both events have a burst duration of the order of 2 ms. The difference in amplitude is certainly due to the material and the energy required for breaking. The

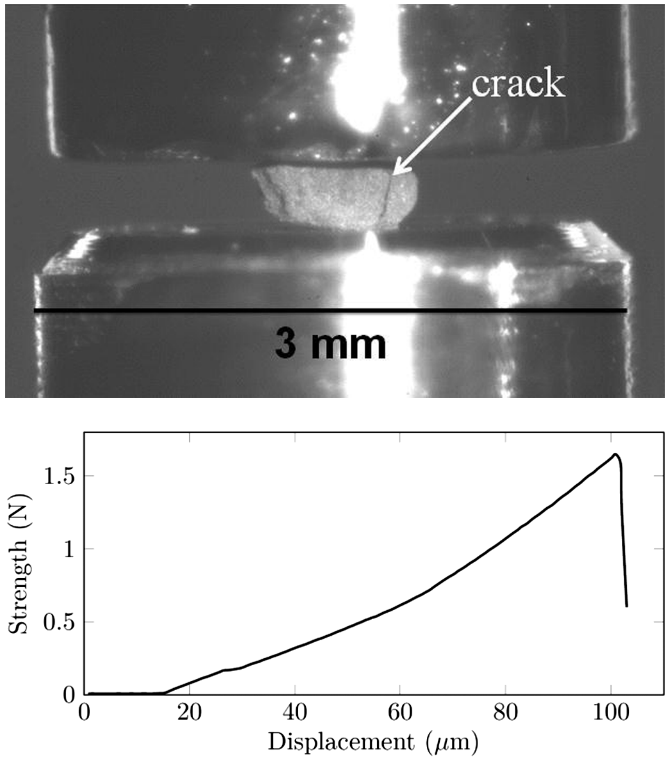

Fig. 8. Illustration of a single crushed UO_2 granule and associated load curve.

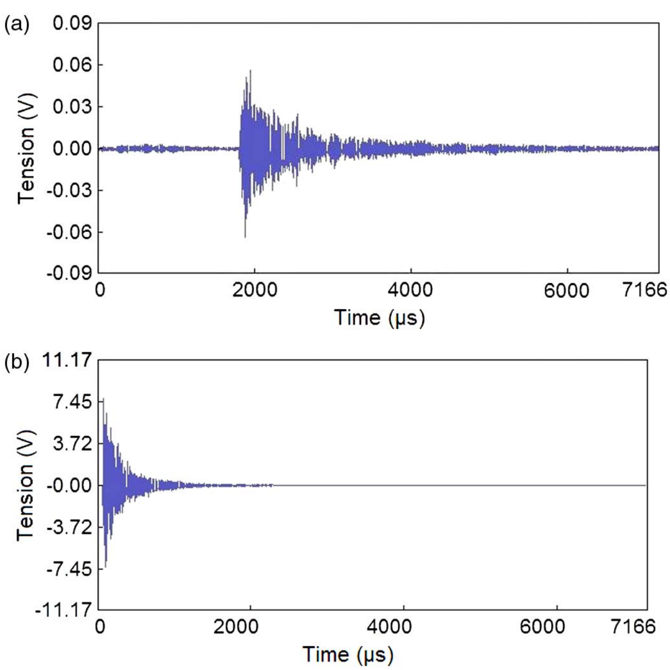

Fig. 9. Burst emitted upon rupture of (a) a single granule: 56 dB and (b) a pencil lead break: 98 dB.

shape of the burst recorded during the rupture of the granule is a typical characteristic of fragmentation.

A batch of 12 granules is thermally consolidated at 1200°C under hydrogen atmosphere. At this temperature, UO_2 starts sintering. Some solid links are then formed, which increases the mechanical strength of the granules. We also crushed those consolidated granules one by one. Table I displays data of both batches: consolidated and non-consolidated granules. Because of significant dispersion, Weibull statistics [12] are used to determine a mean value of breaking load, burst amplitude and burst duration.

TABLE I
MECHANICAL STRENGTH AND ACOUSTIC EMISSION RESULTS OF TWO BATCHES OF GRANULES

Batch	Breaking Load (N)	Burst Amplitude (dB)	Burst Duration (ms)
Non-consolidated granules	1.49 – 0.55*	53 – 17*	5.22 – 5.97*
Consolidated granules	4.59 – 2.41*	69 – 17*	18.76 – 6.09*

* Standard Deviation

As expected, consolidated granules have a higher breaking load than non-consolidated granules, even considering the standard deviation. The rupture stress cannot be accurately calculated because of the cracking surface which is difficult to determine. A signal burst is recorded for all granules at the rupture. For non-consolidated granules, most of the cracks are clearly defined and cross over the granule, which leads to its separation into two parts. For consolidated granules, half of the ruptures occur in the same way as the non-consolidated granules. However, two-thirds of the crushing produces a first crack which seems to stop and then other cracks develop. The reason for this way of cracking must be investigated more thoroughly with granules consolidated at different temperatures and then at different steps of sintering.

Acoustic emission values (Table I) show a trend of increase in burst amplitude and burst duration for consolidated granules. High standard deviations reveal that this trend must be confirmed by carrying out additional tests.

2) Compaction of a Bed of Granules: The press chamber filled by the granules presented in Section II-A is 25 mm in height (filling density equal to 3.3 g/cm^3). A high bed of granules causes a density gradient between the upper part of the compact and the lower part during compaction. The difference between applied stress and transmitted stress, as shown in Fig. 5, clearly reveals this phenomenon. It was explained by Janssen using the example of a grain silo filling [13]. In order to minimize this effect, we must decrease the height of the bed of granules and therefore the number of granules. We choose a larger die with a diameter of 25 mm. That leads to minimizing friction between granules and the die wall.

We record the acoustic emission during compaction of granules presented in Section II-A. As mentioned for the compaction of alumina powders [14], pharmaceutical powders [2] or sand [15], the number of counts increases with the density, i.e., with the stress (Fig. 10).

The cumulative number of counts increases exponentially up to a stress of about 45 MPa. Increasing acoustic emission activity means that fragmentation of the granules and intergranular friction occur. Above 45 MPa, the increase is more pronounced until it reaches a small plateau at 70 MPa. A plateau indicates that no physical mechanism occurs and/or the piezoelectric sensor does not record acoustic waves produced by the potential physical phenomena. When the stress exceeds

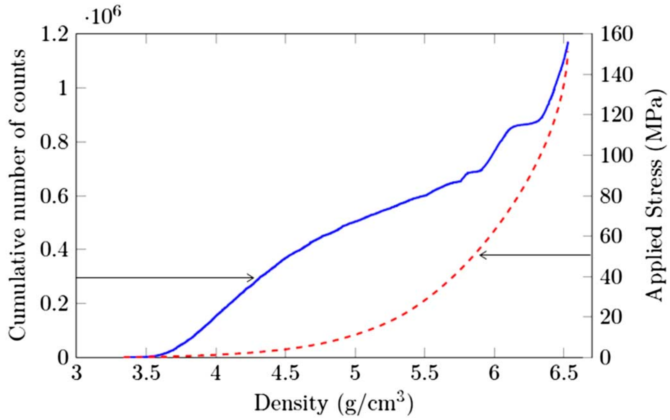

Fig. 10. Cumulative number of hits and applied stress, as a function of the compact density.

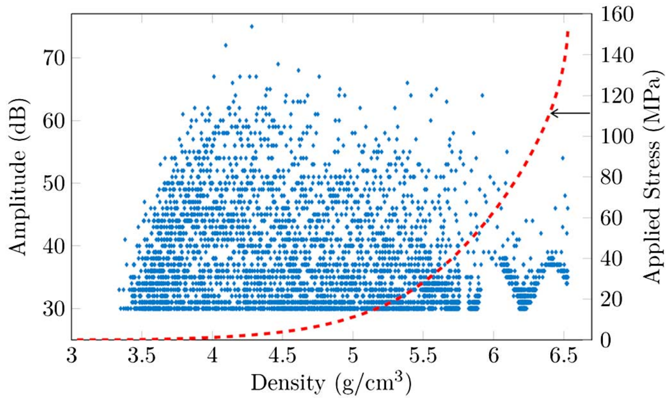

Fig. 11. Maximum amplitude of burst signals and applied stress, as a function of the compact density.

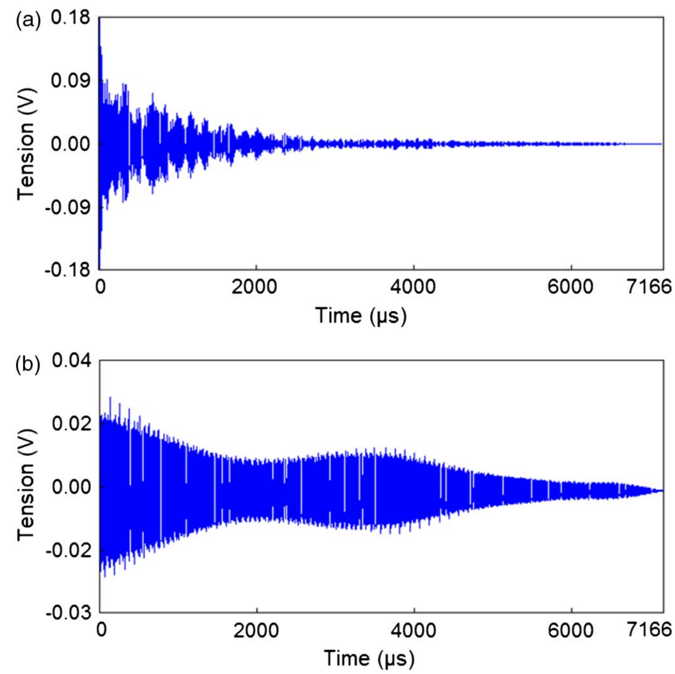

Fig. 12. Typical bursts emitted: (a) below 6.1 g/cm^3–60 MPa, (b) beyond 6.1 g/cm^3–60 MPa.

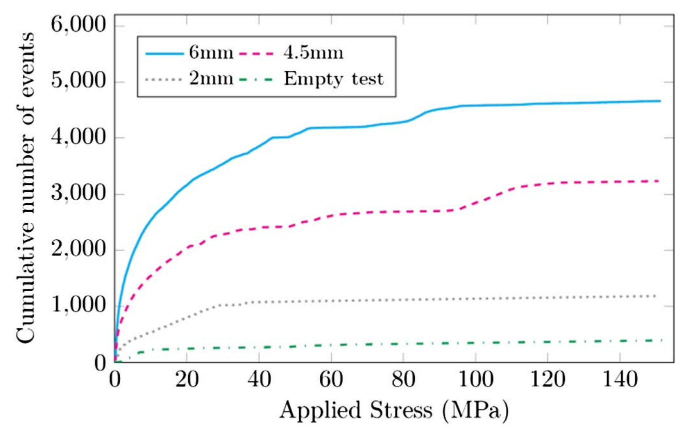

Fig. 13. Cumulative number of events/bursts during the compaction of a bed of granules with three different chamber heights: 6.0 mm, 4.5 mm, 2.0 mm, and during an empty test.

95 MPa, the number of counts again increases drastically. Each blue point plotted in Fig. 11 corresponds to the amplitude of a burst signal, recorded at a given density of the compact. The detection threshold was fixed at 30 dB.

It has been noticed that burst signals of high amplitude appear as soon as a density of 3.4 g/cm^3 (53%) is reached. Beyond 6.1 g/cm^3 (95%) burst amplitude is mainly less than 40 dB. Between 3.4 g/cm^3 and 6.1 g/cm^3, more than 80% of the burst signals, with an amplitude greater than 35 dB, have a shape identical to that recorded for the rupture of a single granule. Fig. 12(a) is a typical burst of this population. They are characteristic of the granule fragmentation.

On the other hand, bursts observed at a stress greater than 60 MPa, which corresponds to a density equal to 6.1 g/cm^3 [Fig. 12(b)], have a very different waveform compared to those characteristic of fragmentation. The mechanism underlying these burst signals has yet to be identified.

We check that the recorded signals are generated by the granules and are not emitted by mechanical or electromagnetic phenomena. Indeed, the compression system is located in a laboratory in which other devices can interfere with the acoustic emission record system. On one hand we record acoustic emission during an empty test which consists in a compression of the upper punch against the lower one up to 150 MPa. Fig. 13 shows that there is a far higher number of events during granule compaction than during the empty test. That means that a significant number of bursts are emitted by granules themselves. Mechanisms responsible for those signals may be: fragmentation of granules, friction between granules and friction between granules and the die wall (however minimized by lubrication).

On the other hand, we compact granules with different bed heights in the die with a diameter of 25 mm. Fig. 13 shows that the number of AE signals increases with the height of the bed, i.e. the number of granules in the die. In fact, the highest bed of granules (6.0 mm) has the highest number of granules.

Fig. 14 presents the evolution between the number of granules in the press chamber and the total number of recorded bursts. Knowing the density of a single granule and the total mass of the material in the press chamber, we calculate the number of granules by assuming that the granules are spherical and their average diameter is 330 μm. Since the number of signals increases

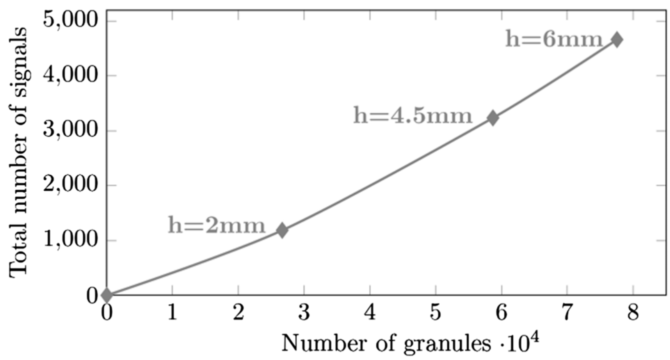

Fig. 14. Evolution of the total number of recorded signals, as a function of the number of granules filled in the press chamber with the height "h".

with the number of granules, the majority of the recorded signal bursts are due to granules, and more specifically, AE is due to granule fragmentations and frictions between them. In our conditions, the distance between the sensor and the bed of granules does not influence acoustic emission recording.

IV. Conclusion

This work examines the evolution of a granular medium controlled in size and mechanical strength during its compaction at various pressures. For UO_2 granules with a 160-500 micrometer size and breaking strength of about 1.5 N, porosity between the granules starts being closed at 300 MPa. Beyond this pressure, the granules are compressed in part on themselves. The decrease in porosity means that granules move by sliding/rotation, which produces friction between them and rupture of whole granules, as well as fragments. These physical mechanisms are visible on the SEM images of compacts manufactured at different pressures. Moreover, these ceramographic sections of compacts show that some granules do not fragment, although the porosity between the granules is not completely filled. They are thus subject to a shear stress weaker than their cohesion. These experimental results are in agreement with the numerical results obtained using a discrete element approach implementing dynamics of contacts [16].

However, this imagery technique cannot be implemented in a shielded cell for fuels containing minor actinides. In order to follow the evolution of the microstructure during the compaction of calibrated particles, the acoustic emission method is proposed.

First we showed that the rupture of granules emits a signal, and that this burst has a typical waveform. We have attributed this waveform to the acoustic signature of fragmentation. We also found these typical waveforms among signals recorded during compaction of a bed of granules. However signals have different waveforms beyond an applied pressure of 60 MPa. The phenomena underlying these burst signals have to be identified. This possible change in mechanism is also observed on the curve of the cumulative number of counts.

We then verified that signals recorded during the compaction of a bed of granules are due to the granules themselves and not to spurious noise. By changing the height of the press chamber, we can vary the number of granules present in the press. We show that, the more granules there are in the press, the more the number of signals recorded during their compaction until 160 MPa is high.

Therefore, acoustic emission is a promising and powerful tool for monitoring the compaction of nuclear calibrated particles through mono-parameter treatments processing together with analysis of the signal waveform.

Acknowledgment

The author would like to thank L. Cao, A. Johnson, and C. Ilgner of the IEEE for their constructive suggestions which improved the paper.

References

[1] A. Hakanen and E. Laine, "Acoustic characterization of a microcrystalline cellulose powder during and after its compression," *Drug Dev. Ind. Pharm.*, vol. 21, no. 13, pp. 1573–1582, 1995.
[2] E. Serris, L. Perier-Camby, G. Thomas, M. Desfontaines, and G. Fantozzi, "Acoustic emission of pharmaceutical powders during compaction," *Powder Technol.*, vol. 128, pp. 296–299, 2002.
[3] S. Eissa, "Condition monitoring of pharmaceutical powder compression during tabletting using acoustic emission," Ph.D dissertation, Brunel University, Uxbridge, U.K., 2003.
[4] E. Rémy, S. Picart, S. Grandjean, T. Delahaye, N. Herlet, P. Allegri, O. Dugne, R. Podor, N. Clavier, P. Blanchart, and A. Ayral, "Calcined resin microsphere pelletization (CRMP): A novel process for sintered metallic oxide pellets," *J. Eur. Cer. Soc.*, vol. 32, pp. 3199–3209, 2012.
[5] J. Danroc, Evolution superficielle et aptitude au compactage des poudres de dioxyde d'uranium, unpublished, Centre d'Etudes Nucléaires de Grenoble, Rapport CEA-R-5185, 1982.
[6] B. Saint-Cyr, "Modélisation des matériaux granulaires cohésifs à particules convexes: Application à la compaction des poudres $d'UO_2$," Ph.D. dissertation, Université Montpellier 2, Montpellier, France, 2011.
[7] M. Renouard, "De la particule au compact: vers une explication du phénomène de clivage des comprimés de paracétamol," Ph.D. dissertation, Compiègne Tech. Univ., Compiègne, France, 2001.
[8] K. Van Der Voort Maarchalk, "Stress relaxation of compacts produced from viscoelastic materials," *Int. J. Pharm.*, vol. 151, pp. 27–34, 1997.
[9] J. Fourcade, "Etude de la mise en forme par pressage uni-axial des poudres de combustible nucléaire," Ph.D. dissertation, Université Montpellier 2, Montpellier, France, 2002.
[10] H. Giesche, "Mercury Porosimetry: a general (practical) overview," *Particle & Particle Syst. Characteriz.*, vol. 23, pp. 9–19, 2006.
[11] G. Kerboul, "Etude de l'endommagement des produits céramiques crus par émission acoustique," Ph.D. dissertation, GEMPPM, INSA, Lyon, Dept. Fuel Stud., CEA Cadarache, Lyon, France, 1992.
[12] W. Weibull, "A statistical distribution function of wide applicability," *ASME J. Appl. Mech.*, pp. 293–297, 1951.
[13] F. M. Mahoney and M. J. Ready, "Applied mechanics modeling of granulated ceramic powder compaction," presented at the Conf. 'Glass and Electronic Ceramics Department, Sandia National Laboratories, Albuquerque, NM, 1995.
[14] T. Kathrina and R. D. Rawlings, "Acoustic studies of the effect of SiC particle reinforcement on the compaction of alumina powder," *J. Eur. Cer. Soc.*, vol. 17, pp. 1157–1166, 1997.
[15] E. Roueche, G. Thomas, L. Perier-Camby, and E. Serris, "Fragmentation de grains de sable. Suivi par émission acoustique et bilans de population," in *Proc. De la poudre au matériau massif*, 2003.
[16] D. H. Nguyen, E. Azéma, F. Radjai, and P. Sornay, "Modélisation numérique de la compaction des milieux granulaires constitués de grains sécables," in *Proc. CIGOS04-05*, Lyon, France, Apr. 2013.